Semicond. Sci. Technol. **24** (2009) 015005 (4pp) doi:10.1088/0268-1242/24/1/015005

Vacancy engineering by He induced nanovoids in crystalline Si

S Kilpeläinen[1], K Kuitunen[1], F Tuomisto[1], J Slotte[1], E Bruno[2], S Mirabella[2] and F Priolo[2]

[1] Department of Applied Physics, Helsinki University of Technology, PO Box 1100, FI-02015 TKK, Finland
[2] MATIS CNR-INFM and Dipartimento di Fisica e Astronomia, Università di Catania, Via S Sofia, I-95123 Catania, Italy

Received 9 October 2008, in final form 30 October 2008
Published 5 December 2008
Online at stacks.iop.org/SST/24/015005

Abstract
Positron annihilation spectroscopy (PAS) in the Doppler broadening mode is used to study the effects of He and B implantation, and subsequent annealing on the vacancy profile of crystalline Si. The existence of two void layers, one consisting of large voids at the projected range (R_p) of He and another containing 'nanovoids' slightly larger than divacancies at roughly halfway between R_p of He and the surface is shown for samples implanted with He. Furthermore, the same nanovoid layer is shown to be absent from samples co-implanted with B, implying that interstitials created during B implantation get trapped in the nanovoids and fill them, thus indicating that the nanovoid layer is behind the hindrance of B diffusion.

1. Introduction

Methods for point defect control in crystalline silicon (c-Si) are becoming more than ever key processes in microelectronic device fabrication because of the ultra-scaled dimensions demanded by the increasing miniaturization [1]. In fact, the realization of ultra-shallow, p+/n junctions typically requires high-dose, low-energy B implantation in c-Si whose main drawback is the drastically enhanced Si self-interstitial (Is) density. Since B diffusion is exclusively mediated by Is in c-Si, transient enhanced diffusion (TED) of the dopant is observed during post-implantation annealing [2], which greatly obstructs dopant confinement attempts. Indeed, the Is excess causes the formation of inactive B-Is clusters (BIC), highly detrimental for any microelectronic application [3, 4]. Thus, a reliable method for controlling the Is excess in c-Si in such conditions is highly demanded, with large compatibility with the well-assessed ion implantation technology.

Recently, some vacancy (V) engineering approaches have been attempted with the idea of pre-emptively elevating the V density of crystalline Si in order to decrease the Is population. In pre-amorphized Si this aim is successfully achieved by using F co-implantation, which gives out a quite stable V excess in the form of nanometer cavities, leading to a significant reduction of B diffusivity in re-crystallized Si [5, 6]. In c-Si Cowern and co-workers have shown that high-energy Si self-implantation generates, in the B co-implanted region, a V supersaturation able to reduce the diffusion of B and to enhance its electrical activation [7–9]. Still, the V excess induced this way will have a limited stability because of the lack of the larger defect complexes able to survive the thermal budget required. Instead, He implantation in c-Si is well known to create large and quite stable cavities at the projected range (R_p), allowing a more durable V excess, but with an undesirable defective region highly influencing the local electrical features [10].

As a promising alternative, nanovoids (2–3 nm in size) have been observed by transmission electron microscopy (TEM) to form after He implantation in c-Si in between the surface and R_p, efficiently acting to reduce the diffusion of co-implanted B and enhancing its electrical activation [11–13]. Peeva *et al* have observed Cu gettering at $R_p/2$ in He-implanted Si which can also be attributed to this nanovoid layer [14]. Larger cavities at R_p are formed too, but correct implant engineering can place them far away from the B doped region, avoiding related detrimental effects [13]. Marcelot *et al* subsequently observed similar B diffusion reduction in the presence of pre-formed larger voids (10–20 nm in size) induced at R_p by He implants and annealed prior to B implantation, suggesting Ostwald ripening between large voids as the source of the V excess [15]. Still, the larger the V clusters, the lower the induced V excess during the ripening and the greater

Table 1. The implantation and annealing parameters for the studied samples.

	He energy (keV)	He fluence (ions cm^{-2})	B energy (keV)	B fluence (ions cm^{-2})	Annealing temperature
#1	80	5×10^{15}	–	–	–
#2	80	3×10^{16}	–	–	–
#3	80	3×10^{16}	12	5×10^{15}	–
#4	80	7×10^{15}	–	–	800 °C
#5	80	1×10^{16}	–	–	800 °C
#6	80	3×10^{16}	–	–	800 °C
#7	80	8×10^{16}	–	–	800 °C
#8	80	1×10^{16}	12	5×10^{15}	800 °C
#9	80	3×10^{16}	12	5×10^{15}	800 °C
#10	80	8×10^{16}	12	5×10^{15}	800 °C

indeed the deviation from the ideal defect-free Si crystal, leading to the favouring of the nanovoids over the bigger V clusters for these microelectronic applications.

Krause-Rehberg *et al* have studied self-implanted Si with positron annihilation spectroscopy (PAS) and confirmed the existence of vacancy clusters at $R_p/2$ [16], and Fedorov *et al* have done the same for He-implanted Si [17] but there is no systematic experimental investigation available either on the formation kinetics or on the dimension of He-implantation induced nanovoids, which form in the track region of He ions above $R_p/2$ and can be well below the TEM detection limit in the size (∼1 nm).

In this work we focus our attention on the formation of open-volume defects in c-Si after He implantation and annealing using PAS in the Doppler broadening mode. With the technique, we measure the momentum of the electrons annihilating with positrons. Valence and core electrons have different momenta, so we are able to determine the type of the annihilating electrons from the data. As open-volume defects lack the core electrons, valence annihilation is dominant in them, and thus it is possible to observe the defects with PAS. From the Doppler broadening data, we observed that open-volume defects are created close to the surface in c-Si just after He implantation, evolving into nanovoids slightly larger than divacancies, upon annealing. While Fedorov *et al* referred to nanocavities in their study [17], the defects observed were considerably larger than those presented in this work. The evolution of these nanovoid defects and the dependence on the He implant fluence and on a further B implantation have been investigated.

2. Experiment

The samples used in this work were from Si (1 0 0) Czochralski wafers, n-type, 1.5-4 Ω cm (corresponding P concentrations 3.4×10^{15}–9.5×10^{15} cm^{-3}). They were implanted with 80 keV He ions ($R_p \sim 600$ nm) at various fluences ranging from 5×10^{15} to 8×10^{16} ions cm^{-2}. In addition to He implantation, some of the samples were implanted with 12 keV B ions ($R_p \sim 50$ nm) at 5×10^{14} ions cm^{-2}. The ion implantation flux was about 1–2 μA cm^{-2}. Three of the samples were measured as-implanted, and the rest had undergone thermal annealing for 10 min at 800 °C after the ion implantation. A summary of the measured samples is presented in table 1. Prior to measurements all samples were etched in HF acid to remove the native oxide which has been shown to skew positron measurement data [18]. All ion implantations and measurements were done at room temperature.

The experiments were performed with a variable energy (0.5–35 keV) slow positron beam by measuring the Doppler broadening of the 511 keV annihilation line [19]. The beam was equipped with two Ge-detectors, each of which has an energy resolution of 1.3 keV at 511 keV. The Doppler broadening was described using the conventional line shape parameters S and W which correspond to the fraction of positrons annihilating with low-energy (valence) and high-energy (core) electrons, respectively. When thermalized positrons are trapped by vacancy-type defects, the reduced local electron density leads to an increase in S and a decrease in W. The energy windows for S and W are typically selected so that the sensitivity to changes in the annihilation environment is at maximum. The S window spans symmetrically across the 511 keV peak and was chosen in this work to include annihilation photon energies fulfilling $|\mathrm{E} - 511\ \mathrm{keV}| < 0.83$ keV. The W regions are defined on both sides of the peak at equal distances from the centre. The W windows were set to $3.00\ \mathrm{keV} < |\mathrm{E} - 511\ \mathrm{keV}| < 7.60$ keV. The W data are not shown since W is mainly used to extract information about the chemical surroundings of defects, which is not relevant in the present work.

3. Results

Figure 1 shows the S parameter as a function of positron implantation energy for samples measured as-implanted (*a*), annealed samples without B (*b*) annealed samples with B (*c*) and a comparison of all three at He fluence of 3×10^{16} ions cm^{-2} (*d*). All S parameter values have been scaled to the value in defect-free Si ($S_{\mathrm{Si}} = 0.523$), and the mean positron implantation depth is also included in the picture. The measured S parameters are superpositions of different positron annihilation states and are given by

$$S = \sum_i n_i S_i, \tag{1}$$

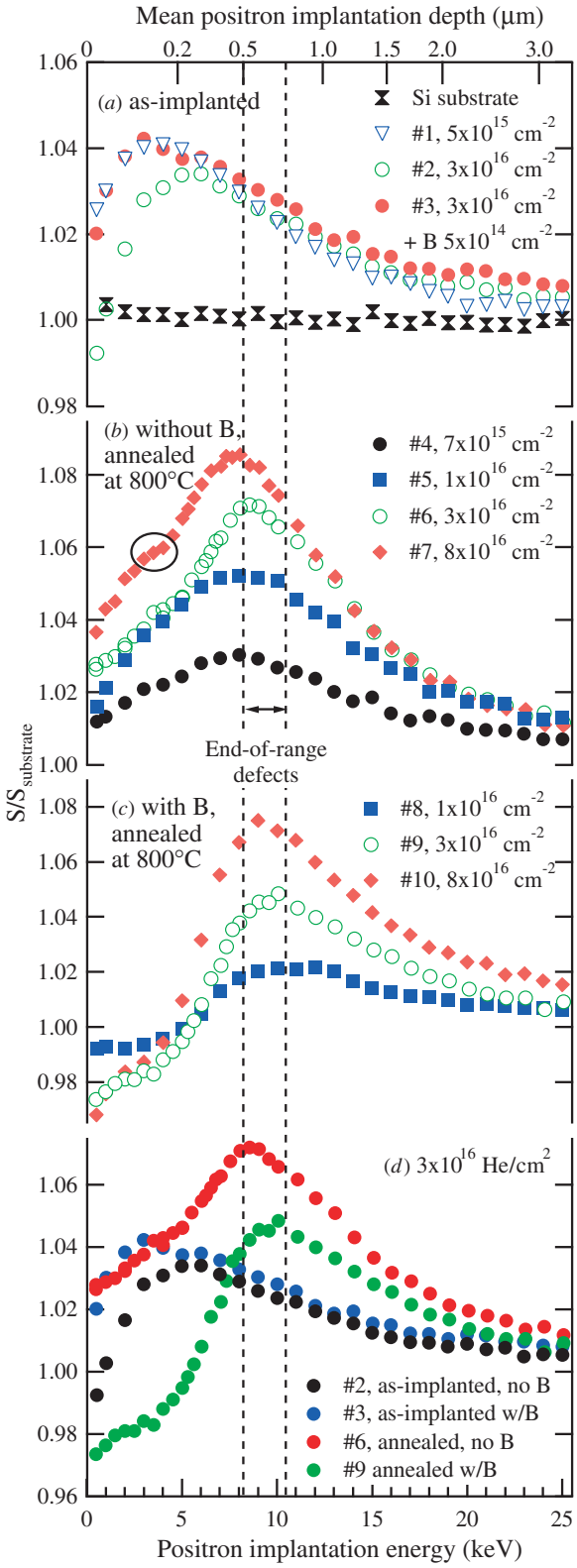

Figure 1. The line shape parameter S as a function of positron implantation energy (depth) for as-implanted (a), annealed (b) and B co-implanted plus annealed (c) samples. Panel (d) compares the as-implanted, annealed and B co-implanted plus annealed cases for samples with identical He fluence (3×10^{16} ions cm^{-2}). All values are scaled to the value of Si substrate. The signal related to the nanovoid layer is circled in panel (b).

(This figure is in colour only in the electronic version)

where n_i are the annihilation fractions in states i, and S_i are the S parameters of these states. In the simplest case, there are only two annihilation states. The Si substrate curve in figure 1a is an example of this. At low energies (<3 keV) most positrons annihilate at the surface, producing a low S parameter. On the other hand, at high energies (>20 keV) it is no longer possible for positrons to diffuse to the surface, and thus all contributions to the S parameter are from the substrate state, which has a higher parameter value than the surface state. At energies between 3 keV and 20 keV the S parameter is a linear combination of the surface and the substrate states according to (1).

The samples measured as-implanted (figure 1(a)) produced S parameter curves with a single peak located at the positron implantation energy of 3–5 keV. The peak is a clear indication that a layer of open-volume defects exists between the surface and R_p of He. The height of the peak implies that the dominant defects in this layer are most likely divacancies ($S_{V_2} = 1.05 \times S_b$, where S_b is the relative S parameter value of defect-free Si bulk)[20]). The slightly lower S parameter close to the surface in one of the curves is explained by incomplete etching of the native oxide as the S parameter in SiO_2 is lower than in Si. A notable feature in the results from as-implanted samples is that the S parameter seems insensitive to the large defects known to be created at R_p of He. The absence of the signal from the end-of-range defects can be explained with He atoms filling the open volume at R_p of the He ions, thus reducing the S parameter value [20].

The S parameter curves for He-implanted and subsequently annealed samples (figure 1(b)) show two distinguishable features: a high peak at positron implantation energies of 8–10 keV and signs of a plateau between the peak area and the surface (at ~3–5 keV). The high peak indicates large vacancy clusters which in this case are end-of-range defects (deep voids) formed at R_p during annealing of the He-implantation-induced defects. The plateau is more interesting as it hints at the existence of a layer of open-volume defects different from those at the end of range. The abrupt change in the slope of the $S(E)$ curve at approximately 4 keV is a clear indication that the diffusion length of the positrons, and hence also the annihilation state and trapping defect species, changes. The positrons implanted in this depth interval are unable to diffuse either to the surface or deeper into the sample and the S parameter corresponds to annihilations in this depth interval. In this case, the normalized S parameter value of 1.06 (for the sample implanted with a He dose of 8×10^{16} ions cm^{-2}) shows that the concentration of vacancies is smaller and also that these vacancies are larger than divacancies. The fact that some of these traps cannot be seen with TEM [11] puts an upper limit on their size, i.e. they are smaller than the end-of-range voids. As the precursors for these 'nanovoids' are the divacancies observed in the as-implanted material, the nanovoids are most likely slightly larger than divacancies, and thus consist of a few missing atoms. Even though the S value in the samples with lower He dose is close to the divacancy value, the defect type cannot be a simple divacancy which is not stable at 800 °C.

For annealed samples implanted with both He and B (figure 1(*c*)), the *S* parameter behaves differently. The end-of-range peaks are present at the projected range but they are lower than those obtained from samples with only He implantation. The difference in the peak height can better be seen in figure 1(*d*). This difference could mean that either the defects at the end of range are smaller or their concentration is lower. The region containing the nanovoids looks completely different for samples implanted with both He and B. The *S* parameter curve below 4 keV is close to that of the Si substrate, and thus positron trapping to the nanovoids is almost nonexistent, indicating that interstitials created during B implantation fill the nanovoids and prevent positron trapping. These results, in good agreement with previous TEM and diffusion results [11], confirm that He-induced nanovoids are highly effective in reducing the Is excess created by ion implantation.

4. Conclusions

In conclusion, we studied how He and B implantation and subsequent annealing affect the defect profile in crystalline Si using positron annihilation spectroscopy in the Doppler broadening mode. The results from samples implanted with only He showed that He implantation and annealing afterwards generate two distinct defect layers in the sample: one at the He projected range and one between R_p and the surface. The layer at R_p contains large voids while the other defect layer consists of nanovoids smaller than the end-of-range deep voids but larger than divacancies. This nanovoid layer is completely missing from the data from samples implanted with both He and B, showing that interstitials which are created during B implantation get trapped in the nanovoids. This result verifies that the nanovoids located close to the surface can be fruitfully applied for diminishing the detrimental effects of ion implantation on B diffusion in Si.

Acknowledgments

This work was partially funded by the Academy of Finland.

References

[1] International Technology Roadmap for Semiconductors (ITRS) 2007 http://www.itrs.net/

[2] Jain S C, Schoenmaker W, Lindsay R, Stolk P A, Decoutere S, Willander M and Maes H E 2002 *J. Appl. Phys.* **91** 8919

[3] Pelaz L, Jaraiz M, Gilmer G H, Gossmann H-J, Rafferty C S, Eaglesham D J and Poate J M 1997 *Appl. Phys. Lett.* **70** 2285

[4] Mirabella S, Bruno E, Priolo F, Salvador D D, Napolitani E, Drigo A V and Carnera A 2003 *Appl. Phys. Lett.* **83** 680

[5] Impellizzeri G, Mirabella S, Priolo F, Napolitani E and Carnera A 2006 *J. Appl. Phys.* **99** 103510

[6] Boninelli S, Claverie A, Mirabella S, Impellizzeri G, Priolo F, Napolitani E and Cristiano F 2006 *Appl. Phys. Lett.* **89** 171916

[7] Cowern N, Smith A, Colombeau B, Gwilliam R, Sealy B and Collart E 2005 Electron Devices Meeting, 2005. IEDM Technical Digest. IEEE Int. p 4

[8] Smith A, Cowern N, Gwilliam R, Sealy B, Colombeau B, Collart E, Gennaro S, Giubertoni D, Bersani M and Barozzi M 2006 *Appl. Phys. Lett.* **88** 082112

[9] Gwilliam R, Cowern N, Colombeau B, Sealy B and Smith A 2007 *Nucl. Instrum. Methods* B **261** 600

[10] Raineri V, Saggio M and Rimini E 2000 *J. Mater. Res.* **15** 1449

[11] Mirabella S, Bruno E, Priolo F, Giannazzo F, Bongiorno C, Raineri V, Napolitani E and Carnera A 2006 *Appl. Phys. Lett.* **88** 191910

[12] Bruno E, Mirabella S, Priolo F, Kuitunen K, Tuomisto F, Slotte J, Giannazzo F, Bongiorno C and Raineri V 2008 *J. Vac. Sci. Technol.* B **26** 386

[13] Bruno E, Mirabella S, Priolo F, Napolitani E, Bongiorno C and Raineri V 2007 *J. Appl. Phys.* **101** 023515

[14] Peeva A, Fichtner P F P, da Silva D L, Behar M, Koegler R and Skorupa W 2002 *J. Appl. Phys.* **91** 69

[15] Marcelot O, Claverie A, Cristiano F, Cayrel F, Alquier D, Lerch W, Paul S, Rubin L, Jaouen H and Armand C 2007 *Nucl. Instrum. Methods* B **257** 249

[16] Krause-Rehberg R, Börner F and Redmann F 2000 *Appl. Phys. Lett.* **77** 3932

[17] Fedorov A V, van Veen A, Schut H and Rivera A 1999 *Nucl. Instrum. Methods* B **148** 289

[18] Sihto S-L, Slotte J, Lento J, Saarinen K, Monakhov E, Kuznetsov A and Svensson B 2003 *Phys. Rev.* B **68** 115307

[19] Saarinen K, Hautojärvi P and Corbel C 1998 *Identification of Defects in Semiconductors* ed M Stavola (New York: Academic)

[20] Kauppinen H, Corbel C, Skog K, Saarinen K, Laine T, Hautojärvi P, Desgardin P and Ntsoenzok E 1997 *Phys. Rev.* B **55** 9598